Spatial structure of scattered radiation in a loop parametric oscillator utilizing a photorefractive crystal

A. A. Zozulya, S. A. Korol'kov, Yu. S. Kuz'minov, A. V. Mamaev, and V. V. Shkunov

Institute of Problems in Mechanics, Academy of Sciences of the USSR, Moscow

Detailed experimental investigations were made of the structure of the scattered radiation in a self-pumped loop parametric oscillator utilizing a photorefractive crystal. The experimental results were compared with the predictions of a three-dimensional theoretical model.

1. INTRODUCTION

In many self-pumped four-wave phase conjugation systems proposed and implemented in the last few years scattered radiation is generated in the field of noncollinear pump waves. A typical example is a loop parametric oscillator (Fig. 1) in which a pump beam 2 passes through a nonlinear medium and is returned, by an external optical feedback loop, back to the medium (as beam 4) and intersects itself. Under certain conditions it is found that an excitation (absolute) instability which develops in this geometry gives rise to the scattered radiation beams 1 and 3. The scattered beam 3 travels opposite to the pump beam 4 and, after traversing the feedback loop, is transformed into the beam 1 which propagates opposite to the pump beam 2. The pairs of the scattered and pump beams 1, 4 and 2, 3 form a nonlinear refractive-index grating in the medium. Diffraction of the pump beams by this grating enhances the scattered beams and closes the feedback loop giving rise to the absolute instability.

Such a loop oscillator had been realized experimentally in liquids utilizing stimulated Brillouin scattering[1] and also in photorefractive[2] and liquid[3] crystals. A theoretical description of such an oscillator by one-dimensional models has been developed quite fully because of the simplicity of these models.[2,4,5] However, one-dimensional models represent only the initial stage of a theoretical interpretation. Self-consistent three-dimensional models are needed to determine the structure of the scattered radiation and to develop criteria for selection of the phase-conjugate component and of the quality of phase conjugation. Models of this kind describing generation of scattered radiation in the field of noncollinear pump waves had been proposed in Refs. 6 and 7, which made it possible to go over from empirical construction of self-pumped four-wave phase conjugation systems to a purposeful investigation of these systems and a quantitative comparison of the theory with experiment.

Here we report a detailed experimental investigation of the structure of the scattered radiation in the geometry of a self-pumped loop parametric oscillator and we shall compare the results with predictions of the models proposed in Refs. 6 and 7. The rest of the paper is organized as follows: Sec. 2 provides a theoretical description of a loop parametric oscillator based on the results of Refs. 6 and 7, Sec. 3 reports the experimental results, and Sec. 4 gives the conclusions.

2. THEORY

Let us assume that the beams intersect in the (x', y') plane. Then, the system of reduced equations for the slowly varying amplitudes of the scattered beams 1 and 3 in a photorefractive medium, neglecting pump depletion is

$$\left(\cos\theta\frac{\partial}{\partial x'}+\sin\theta\frac{\partial}{\partial y'}-\frac{i\Delta_{\perp,1}}{2k_0}\right)A_1(\mathbf{r})=\nu A_4(\mathbf{r}),$$

$$\left(-\cos\theta\frac{\partial}{\partial x'}+\sin\theta\frac{\partial}{\partial y'}-\frac{i\Delta_{\perp,3}}{2k_0}\right)A_3(\mathbf{r})=\nu A_2(\mathbf{r}), \quad (1)$$

$$\nu=(\gamma/I_T)(A_1A_4^*+A_2^*A_3).$$

Here, 2θ is the angle between the beams 2 and 3 in the nonlinear medium,

$$\Delta_{\perp,1(3)}=\left(\mp\sin\theta\frac{\partial}{\partial x'}+\cos\theta\frac{\partial}{\partial y'}\right)^2+\frac{\partial^2}{\partial z'^2}$$

are the transverse Laplacians, ν is the amplitude of the nonlinear refractive-index grating, γ is the coupling coefficient, and

$$I_T=|A_2(\mathbf{r})|^2+|A_4(\mathbf{r})|^2, \quad \mathbf{r}=(x', y', z').$$

The coupling coefficient γ allows for a possible detuning of the frequency of the scattered beams from that of the pump beams. In the case of a purely diffuse response of the medium, we have $\gamma = \gamma_0/(1 - i\delta)$. Here, γ_0 is the real coupling parameter and $\delta = \omega\tau$, where ω is the frequency offset between the scattered and pump waves, and $\tau(\mathbf{r}) \sim \approx I_T^{-1}(\mathbf{r})$ is the relaxation time of the nonlinear medium.

The system (1) should be supplemented by the following boundary conditions, corresponding to the specified input intensity of the pump beam 2 and zero intensity of the scattered beam 3:

$$A_{2,\,in}(\mathbf{r})=A_0(\mathbf{r}), \quad A_{3,\,in}(\mathbf{r})=0, \quad (2a)$$

and the transformation of the beams 2, 3 into the beams 3, 1 in the course of propagation along the feedback loop:

$$A_{4,\,in}(\mathbf{r})=\hat{L}A_{2,\,out}(\mathbf{r}), \quad A_{1,\,in}(\mathbf{r})=\hat{L}^{-1}A_{3,\,out}(\mathbf{r}). \quad (2b)$$
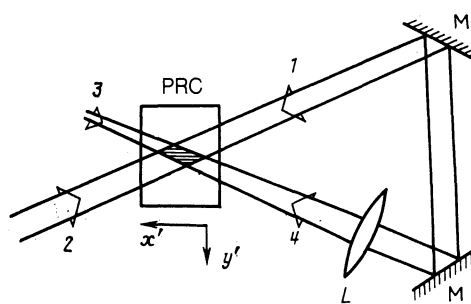

FIG. 1. Schematic diagram of a loop parametric oscillator: 2), 4) primary and secondary pump beams; 1), 3) scattered beams; L is the system of lenses; M are rotatable mirrors; PRC is a photorefractive crystal.

Here, $\hat{L}$ and $\hat{L}^{-1}$ are the relevant transformation operators. The plane (x',y') of the intersection of the beams and the direction perpendicular to this plane have qualitatively different roles in the operation of the loop oscillator. We can reveal this difference by assuming that the feedback loop, of length L, is formed by a system of plane mirrors and two cylindrical lenses. A cylindrical lens with a focal length $f_{\|}$ is located at a distance $L_{1,\|}$ from the crystal along the direction of the pump beam and it transforms the radiation in the beam-intersection plane. Another cylindrical lens, with a focal length $f_\perp$, is located at a distance $L_{1,\perp}$ from the crystal and transforms the beams propagating in the direction perpendicular to the intersection plane. Consequently, the boundary conditions of Eq. (2b) can be written in the form

$$A_{4,in}(\rho_\|,\rho_\perp)=\frac{k_0 T^{1/2}}{2\pi i (L_{eff,\|}L_{eff,\perp})^{1/2}}\int\int d\rho_\|{}' \, d\rho_\perp{}' A_{2,out}(\rho_\|{}',\rho_\perp{}')$$

$$\times \exp\left\{\frac{ik_0}{2}\left[\frac{\rho_\|^2}{L_{2,\|}}+\frac{\rho'^2}{L_{1,\|}}-\frac{L_{2,\|}}{L_{1,\|}L_{eff,\|}}\left(\rho_\|{}'+\frac{L_{1,\|}}{L_{2,\|}}\rho_\|\right)^2\right.\right.$$

$$\left.\left.+\frac{\rho_\perp^2}{L_{2,\perp}}+\frac{\rho_\perp'^2}{L_{1,\perp}}-\frac{L_{2,\perp}}{L_{1,\perp}L_{eff,\perp}}\left(\rho_\perp{}'+\frac{L_{1,\perp}}{L_{2,\perp}}\rho_\perp\right)^2\right]\right\}. \quad (3)$$

Here, $\rho_\|$ and $\rho_\perp$ are the transverse (relative to the direction of propagation of the beams) coordinates in the beam-intersection plane (index $\|$) and at right-angles to this plane (index $\perp$); $L_{2,k}=L-L_{1,k}$, $L_{eff,k}=L-L_{1,k}L_{2,k}/f_k$ ($k=\|,\perp$) and $T\leqslant 1$ is the transmission coefficient of the feedback loop. The boundary conditions for the scattered beams 1 and 3 follow from Eq (3) if we make the substitution $L_{1(2)}\rightarrow L_{2(1)}$.

We represent the amplitude of the interacting beams A_j ($j=1$–4) in the form

$$A_j(\rho_\|,\rho_\perp)=B_j(\rho_\|,\rho_\perp)\exp\left[\frac{ik_0}{2}\left(\frac{\rho_\|^2}{R_{j,\|}}+\frac{\rho_\perp^2}{R_{j,\perp}}\right)\right], \quad (4)$$

where $R_{j,\|}$ and $R_{j,\perp}$ are the radii of curvature of the wavefront, and B_j are the complex amplitudes which carry all the other information about the beams. The relationships described by Eq. (4) are derived in a local coordinate system for each beam, i.e., for the beams 1 and 2 we have $\rho_\|=y'\cos\theta-x'\sin\theta$, whereas for the beams 3 and 4 we have $\rho_\|=y'\cos\theta+x'\sin\theta$), and for all the beams we have $\rho_\perp=z'$.

Consider the case when the optics in the feedback loop maps the region of overlap (intersection) of the beams on itself, i.e., when the effective length of the feedback loop is small: $L_{eff,\|}$, $L_{eff,\perp}\ll k_0a^2$, where a is the characteristic scale of the change in the complex amplitudes B_j. The boundary conditions of Eq. (3) then lead to the following relationships governing the radii of curvature and the amplitudes B of the pump beams:

$$R_{4,k}=L_{eff,k}\left(1-\frac{L_{1,k}}{f_k}-\frac{1}{\alpha_k}\right)^{-1},$$

$$\alpha_k=1-\frac{L_{2,k}}{f_k}+\frac{L_{eff,k}}{R_{2,k}}, \qquad k=\|,\perp, \quad (5)$$

$$B_4(\rho_\|,\rho_\perp)=\left(\frac{T}{\alpha_\|\alpha_\perp}\right)^{1/2}B_2\left(\frac{\rho_\|}{\alpha_\|},\frac{\rho_\perp}{\alpha_\perp}\right).$$

According to the system (5), the propagation of radiation in the feedback loop may be described by geometric

optics. The transverse structure of the pump beam 2 exhibits a scale transformation in the beam intersection plane with the scaling transformation coefficient $\alpha_\|$ and in the transverse direction, with the coefficient $\alpha_\perp$. From the practical point of view the scaling coefficient $\alpha_\|$ is simply equal to the ratio of the width of the pump beam 4 in the plane of intersection to the width of the pump beam 2. For $|\alpha_\||<1$, the pump beam 4 is narrower than the pump beam 2, while for $|\alpha_\||>1$ the reverse is true. This applies also to the scaling coefficient $\alpha_\perp$, but at right-angles to the beam-intersection plane.

By analogy with the system (5), we can write down the following expressions for the scattered radiation beams:

$$R_{1,k}=L_{eff,k}\left(1-\frac{L_{2,k}}{f_k}-\frac{1}{\beta_k}\right)^{-1},$$

$$\beta_k=1-\frac{L_{1,k}}{f_k}+\frac{L_{eff,k}}{R_{3,k}}, \qquad k=\|,\perp, \quad (6)$$

$$B_{1,in}(\rho_\|,\rho_\perp)=\left(\frac{T}{\beta_\|\beta_\perp}\right)^{1/2}B_{3,out}\left(\frac{\rho_\|}{\beta_\|},\frac{\rho_\perp}{\beta_\perp}\right).$$

Note that the radii of curvature of the wavefront of the pump beam 2 are given by the boundary condition of Eq. (2a), which makes it possible to determine them for the pump beam 4 from Eq. (5), but the radii of curvature of the wavefronts of the scattered beams are unknown at this stage. We can find them bearing in mind that the nolinear grating of the refractive index v of Eq. (1) can be formed effectively only if the strong phase dependences in the terms $A_1A_4^*$ and $A_2^*A_3$, associated with the radii of curvature, are identical. Allowance for this circumstance perpendicular to the beam-intersection plane gives

$$R_{1,\perp}^{-1}+R_{2,\perp}^{-1}-R_{3,\perp}^{-1}-R_{4,\perp}^{-1}=0. \quad (7)$$

The system of equations (5)–(7) has two solutions. For the first of them, we have

$$R_{1,\perp}=-R_{2,\perp}, \quad R_{3,\perp}=-R_{4,\perp}, \quad \beta_\perp=1/\alpha_\perp, \quad (8)$$

and for the second, we obtain

$$R_{1,\perp}=L_{eff,\perp}\left(1-\frac{L_{2,\perp}}{f_\perp}-\frac{1}{\alpha_\perp}\right)^{-1},$$

$$R_{3,\perp}=L_{eff,\perp}\left(-1+\frac{L_{1,\perp}}{f_\perp}+\alpha_4\right)^{-1}, \quad \beta_\perp=\alpha_\perp. \quad (9)$$

The conditions for cancellation of the strong phase dependences in the beam-intersection plane are found to be different from those given by Eq. (7) because of the noncollinearity of the beams:

$$(y'\cos\theta-x'\sin\theta)^2(R_{1,\|}^{-1}+R_{2,\|}^{-1})$$

$$-(y'\cos\theta+x'\sin\theta)^2(R_{3,\|}^{-1}+R_{4,\|}^{-1})=0 \quad (10)$$

and they lead to the unique solution

$$R_{1,\|}=-R_{2,\|}, \quad R_{3,\|}=-R_{4,\|}, \quad \beta_\|=1/\alpha_\|. \quad (11)$$

A solution analogous to Eq. (9) can be obtained only for very thin media and small angles θ of convergence of the beams, such that

$$k_0\,dl\theta\sum_{j=1}^{4}R_{j,\|}^{-1}\ll 1,$$

where d is the characteristic beam diameter and l is the characteristic length of the nonlinear medium. The above inequality is practically impossible to satisfy under typical experimental conditions.

The solution described by Eqs. (8) and (11) is of the greatest interest, because in this case the fast phase component of the scattered radiation beams, related to the radii of curvature of their wavefronts, is phase-conjugated relative to the pump beams. We shall analyze in detail this solution and determine the range of its existence, as well as the conditions for going over from this solution to the solution described by Eqs. (9) and (11).

After explicit separation of the radii of curvature of the beam wavefronts and of the image-carrying amplitudes B_j, we can rewrite the system (1) in the form of equations for B_j. We assume that the characteristic length of diffraction spreading $k_0 a^2$ of the amplitudes B_j exceeds the characteristic length of the interaction region l: $k_0 a^2 \gg l$. This means that the diameters of the interacting beams do not change significantly within the length of the interaction region and that we can ignore the transverse Laplacians $\Delta_{1(3)}$ in the equations for B_j.

We shall now replace the coordinate system (x', y', z') with a new system (x,y,z):

$$x = -x' \sin\theta - y' \cos\theta, \quad y = x' \sin\theta - y' \cos\theta, \quad z = z'.$$

In the new coordinate system the pump beam 2 propagates along the x axis and the pump beam 4 along the y axis. The beam diameters are not affected by the transformation to the new coordinate system. The system of equations for the amplitudes B_j in the new system becomes

$$\frac{\partial}{\partial x} B_1(x,y,z) = -\frac{\gamma}{I_T \sin 2\theta}(B_1 B_4^* + B_2^* B_3)B_4,$$

$$\frac{\partial}{\partial y} B_3(x,y,z) = -\frac{\gamma}{I_T \sin 2\theta}(B_1 B_4^* + B_2^* B_3)B_2, \quad (12)$$

and the boundary conditions are written as follows:

$$B_4(x,z) = \left(\frac{T}{\alpha_\| \alpha_\perp}\right)^{1/2} B_2\left(\frac{x}{\alpha_\|}, \frac{z}{\alpha_\perp}\right),$$

$$B_{1, \, in}(y, \, z) = (T\alpha_\| \alpha_\perp)^{1/2} B_{3, \, out}(\alpha_\| y, \, \alpha_\perp z), \quad (13)$$

$$B_{3, \, in}(x, \, z) = 0.$$

In the case of the striction or thermal nonlinearity, when the denominators of the right-hand sides of the system (12) do not include the intensity I_T, we can obtain their analytic solutions for an arbitrary amplitude of the injected pump beam $B_2(y,z)$ (Ref. 6). In the case of photorefractive media when the amplitude B_2 has an arbitrary value, these equations can be solved only approximately.[7] We can avoid cumbersome formulas related to finding the approximate solutions by considering the special case of an injected pump beam with a square cross section $2d \times 2d$ in a constant distribution of the intensity (phase-modulated pumping): $|B_2(y,z)| = $ const if $|y|, |z| \leqslant d$ and $|B_2(y,z)| = 0$ in the opposite case.

We introduce a function $f(x,y,z)$ proportional to the amplitude of the beam 3:

$$B_3(x,y,z) = B_4^*(x,z)f(x,y,z)$$

$$\times \exp\left\{-\frac{\gamma}{(1+q)\sin 2\theta}[qx+y+d(1+q\alpha_\|)]\right\}. (14)$$

The amplitude of the beam 1 can then be expressed in terms of the function f:

$$B_1(x,y,z) = -\frac{\sin 2\theta}{\gamma}(1+q)B_2^*(y,z)\frac{\partial}{\partial y}f(x,y,z)$$

$$\times \exp\left\{-\frac{\gamma}{(1+q)\sin 2\theta}[qx+y+d(1+q\alpha_\|)]\right\}, \quad (15)$$

where $q = T/\alpha_\| \alpha_\perp$ is the ratio of the intensities of the pump beams.

The substitution of Eqs. (14) and (15) into Eq. (12) leads to the following equation for the function $f(x,y,z)$:

$$\frac{\partial^2}{\partial x \, \partial y} f(x,y,z) - q\left[\frac{\gamma}{(1+q)\sin 2\theta}\right]^2 f = 0, \quad (16)$$

subject to the boundary conditions that follow from Eqs. (13)–(15):

$$f(x, \, d, \, z) = 0, \quad (17)$$

$$\frac{\partial}{\partial y}f(\alpha_\| d, y, z) = -\frac{\gamma T}{(1+q)\sin 2\theta}f(\alpha_\| y, -d, \alpha_\perp z)$$

$$\times \exp\left\{\frac{\gamma}{(1+q)\sin 2\theta}[(y+d)(1-q\alpha_\|)+2q\alpha_\| d]\right\}.$$

The solution of Eq. (16) is obtained by the Riemann method allowing for the first boundary condition of Eq. (17), which gives the expression (compare with Ref. 6)

$$f(x,y,z) = -\int_y^d dy' \frac{\partial}{\partial y'}f(\alpha_\| d, y', z)v(x, y, \alpha_\| d, y'), \quad (18)$$

where

$$v(x,y,x',y') = I_0\left(\frac{2\gamma}{(1+q)\sin 2\theta}[q(x'-x)(y'-y)]^{1/2}\right),$$

and I_0 is a modified Bessel function.

The substitution of the second boundary condition from the system (17) into Eq. (18) gives an expression relating the function f at an arbitrary point in the interaction point to its value at the boundary:

$$f(\alpha_\| x, \, -d, \, \alpha_\perp z) = \Psi(x, \, z).$$

Assuming $y = -d$ in the above expression we obtain an integral equation for the function Ψ (Ref. 6):

$$\Psi(x,z) = \frac{\Gamma T}{2(1+q)d}\int_{-d}^d dx' \, \Psi(x', \alpha_\perp z)$$

$$\times I_0\left(\frac{\Gamma}{1+q}\left[\alpha_\| q\left(1-\frac{x}{d}\right)\left(1+\frac{x'}{d}\right)\right]^{1/2}\right)$$

$$\times \exp\left\{\frac{\Gamma}{2(1+q)}\left[\left(1+\frac{x'}{d}\right)(1-q\alpha_\|)+2q\alpha_\|\right]\right\}. \quad (19)$$

Here, $\Gamma = \Gamma_0/(1-i\delta) = 2\gamma d/\sin 2\theta$, where Γ_0 is the real value of the gain representing convective amplification of the scattered radiation and δ is the dimensionless form of the frequency offset between the scattered and pumped beams.

Equation (19) has a solution only for a discrete set of the eigenvalues Γ_0 and δ. Solutions of this kind [representing eigenfunctions of Eq. (19)] determine modes of the investigated loop oscillator. The eigenvalues Γ_0 and δ govern, respectively, the thresholds and frequency shifts of these modes. The spatial structure of the scattered radiation

beams can be found for a specific mode using the relationships (14), (15), and (18), (19) if the solution of Eq. (19) is known.

The modes of the investigated oscillator can be labeled by three indices n, m, and l (n, m, and l are all nonnegative integers). The first two indices will be called transverse, because they label modes with different transverse structures of the scattered radiation field in the plane of intersection (n) and at right-angles to this intersection (m). The third index (l) determines the frequency offset between the scattered and pump beams. It follows from Eq. (19) that the coordinates in the beam-intersection plane are not equivalent to those in the perpendicular direction. In fact, Eq. (19) is an integral equation in terms of the coordinates in the beam-intersection plane, whereas along the coordinate z the relationship represents the nonlocal point mapping $\alpha_\perp z \to z$. The difference is manifested also in the functional dependence (19) on the parameters $\alpha_\perp$ and $\alpha_\parallel$. Since we have $\alpha_\parallel q = T/\alpha_\perp$, the parameter $\alpha_\parallel$ occurs in Eq. (19) only in the combination with $\Gamma/(1 + q)$, i.e., it simply renormalizes the effective magnitude of the nonlinearity, whereas the parameter $\alpha_\perp$ occurs explicitly in Eq. (19).

Equation (19) was derived using the boundary conditions of Eq. (13), which follow from Eq. (8), and correspond to $\beta_\perp = 1/\alpha_\perp$. The second solution of Eq. (8) [given by Eq. (9)] corresponds to $\beta_\perp = \alpha_\perp$ and leads to the following boundary conditions for the scattered beams [compare with Eq. (13)]:

$$B_{1,\,in}(y,\,z) = (T\alpha_\parallel/\alpha_\perp)^{1/2} B_{3,\,out}(\alpha_\parallel y,\,\alpha_\perp^{-1} z),$$

and also to an integral equation which differs from Eq. (19) because it represents the point mapping $\alpha_\perp^{-1} z \to z$. The nonlocal mappings $\alpha_\perp z \to z$ and $\alpha_\perp^{-1} z \to z$ are encountered in the theory of unstable laser resonators; they describe two modes —converging and diverging—which in principle can exist in such resonators. It is known[8] that only the diverging mode is stable and can be found experimentally. For $\alpha_\perp < 1$, the mapping $\alpha_\perp z \to z$ is diverging, whereas $\alpha_\perp^{-1} z \to z$ is covergent, while the reverse is true for $\alpha_\perp > 1$. This means that the solutions of Eq. (19) corresponding to generation of a scattered beam with the radius of curvature of the wavefront phase-conjugated relative to the pump beam are obtained only for $\alpha_\perp < 1$. The scattered radiation generated by a loop mirror for $\alpha_\perp > 1$, is not phase-conjugated relative to the pump and the radius of curvature of its wavefront in the direction perpendicular to the beam-intersection plane is described by Eq. (9).

In an analysis of the solutions of Eq. (19) we note that in the present case of constant-intensity pumping the mode structure of the scattered beams is particularly simple along the z axis:

$$\Psi^{(n,\,m,\,l)}(x,\,z) = \Phi^{(n,\,m,\,l)}(x) z^m.$$

The function $\Phi^{(n,m,l)}(x)$ can be represented as a power series:

$$\Phi^{(n,m,l)}(x) = \sum_{k=0}^{\infty} F_k^{(n,m,l)} \left[\frac{\Gamma^{(n,m,l)}}{2(1+q)}\left(1 - \frac{x}{d}\right)\left(\frac{T}{\alpha_\perp}\right)^{1/2} \right]^k \frac{1}{k!}. \quad (20)$$

The coefficients $F_k^{(n,m,l)}$ satisfy the following system of algebraic equations:

$$F_i = \sum_{j=0}^{\infty} a_{ij} F_j,$$

$$a_{ij} = \frac{T^{1/2}}{i!j!} \alpha_\perp^{m+1/2} \exp\left[\frac{\Gamma T}{\alpha_\perp(1+q)} \right]\left[\frac{\Gamma T^{1/2}}{\alpha_\perp^{1/2}(1+q)} \right]^{i+j+1}$$

$$\times \int_0^1 d\eta\, \eta^i (1-\eta)^j \exp\left[\frac{\Gamma\eta}{1+q}\left(1 - \frac{T}{\alpha_\perp}\right)\right]. \quad (21)$$

Let us exhibit the structure of the solutions of Eq. (21) in the limit of low values of the transmission coefficient of the feedback loop $|\Gamma^2 T/\alpha_\perp| < 1$. The first few families of the solutions generated by Eq. (21) are:

$$T\alpha_\perp^m \exp(\Gamma^{(0,\,m,\,l)}) = 1,$$
$$\Phi^{(0,m,l)}(x) = 1 + \frac{T}{2\alpha_\perp}[\Gamma^{(0,m,l)}]^2\left(\frac{x}{d}\right) + \ldots \approx 1; \quad (22)$$

$$T^2\alpha_\perp^{m-1}\exp(\Gamma^{(1,m,l)}) = -1,$$
$$\Phi^{(1,m,l)}(x) = 1 - \Gamma^{(1,m,l)}\frac{x}{2d} + \ldots \approx \frac{x}{d}; \quad (23)$$

$$T^3\alpha_\perp^{m-2}\exp(\Gamma^{(2,m,l)}) = 1,$$
$$\Phi^{(2,m,l)}(x) = 1 - \Gamma^{(2,m,l)}\frac{x}{d}$$
$$+ \frac{1}{2}(\Gamma^{(2,m,l)})^2\left(\frac{x}{2d}\right)^2 + \ldots \approx \left(\frac{x}{d}\right)^2. \quad (24)$$

The lasing thresholds Γ_0 and the frequency shifts δ of the families of $(0,m,l)$ modes are determined by the first of the relationships in the system (22), the solution of which gives

$$\Gamma_0^{(0,m,l)} = (1 + \delta_{(0,m,l)}^2)\ln(1/T\alpha_\perp^m),$$
$$\delta_{(0,\,m,\,l)} = \pm 2\pi l/\ln(1/T\alpha_\perp^m). \quad (25)$$

The lasing thresholds and the frequency shifts of the $(1,m,l)$ and $(2,m,l)$ modes are found from Eqs. (23) and (24) in a similar manner.

The asymptotic expressions (22)–(25) and analysis of Eq. (19) generally show that the modes with a nonzero frequency shift ($l \neq 0$) and the higher transverse modes in the beam-intersection plane ($n \neq 0$) have high excitation thresholds. The greatest interest lies in the low-threshold family of $(0,m,0)$ modes with zero frequency shifts and approximately the same structure in the beam-intersection plane, but with different structures at right-angles to this plane. The thresholds of the first few modes are plotted in Fig. 2 as a
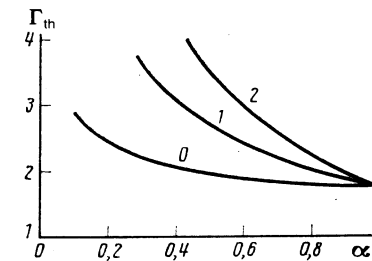

FIG. 2. Dependence of the excitation thresholds of the first three transverse $(0, m, 0)$ modes on $\alpha_\perp$ in the case when $\alpha_\parallel = 1$ and $T = 0.3$. The numbers alongside the curves represent the mode index m.

function of the scaling coefficient $\alpha_\perp$ on the assumption that $\alpha_\| = 1$ and $T = 0.3$.

The different transverse modes correspond to the different quality of the phase-conjugation process, which is assumed to be described by the overlap integral

$$H = \left(\iint d\mathbf{r}_\perp \, A_{2,in} A_{1,out} \right)^2 \bigg/ \iint d\mathbf{r}_\perp |A_{2,in}|^2 \iint d\mathbf{r}_\perp |A_{1,out}|^2,$$

where $A_{2,in}$ is the input amplitude of the pump beam and $A_{1,out}$ is the output amplitude of the scattered beam; the integration in the above expression is carried out over the transverse cross sections of the beams. The input amplitude of the pump beam is determined by the boundary conditions, whereas the output amplitude of the scattered beam is calculated using Eqs. (14), (15) and (18), (19) subject to Eqs. (8) and (11). The overlap integral is defined so that the ideal phase conjugation process corresponds to $H = 1$. In any real situation we have $H < 1$ and its value gives a quantitative measure of the phase-conjugation quality.

Calculation of the overlap integral in the model of a loop oscillator with a striction nonlinearity[9] shows that in the case of the lowest (0,0,0) mode the overlap integral is on the average within the range 50–80%, depending on the profile of the pump beam, on the transmission coefficient T of the feedback loop, etc. In the present photorefractive nonlinearity case the quality of phase conjugation should be somewhat higher because the occurrence of the intensity in the denominator of the expression for the refractive-index grating of Eq. (1) smooths out the profile of the scattered radiation and makes it closer to the profile of the pump beam. The quality of phase conjugation increases with the parameter $\alpha_\perp$. The higher modes correspond to a much lower quality of phase conjugation. The angular divergence of the higher modes transverse to the beam-intersection plane is greater than the divergence of the fundamental mode and increases with the index m. From the point of view of the quality of phase conjugation it is preferable to ensure that the scaling coefficients $\alpha_\perp$ and $\alpha_\|$ are close to unity, but then—in principle—we may expect excitation of several transverse modes because of the proximity of their thresholds (Fig. 2).

The above analysis shows that selection of the phase-conjugated component in the beam-intersection plane occurs automatically because of the noncollinearity of the interacting beams, which establishes an integral coupling between them [see Eq. (19)]. Compression of the secondary pump beam ($\alpha_\perp < 1$) is necessary only for the selection of the phase-conjugated component perpendicular to the beam-intersection plane. The condition $\alpha_\perp < 1$ may be avoided by some method which ensures "mixing" of the coordinates of the beams in the beam-intersection plane and perpendicular to this plane. This can be ensured, for example, by rotating the transverse cross section of the beam in the course of its passage along the feedback loop by an angle different from zero and from 180°, but without altering the direction of the beam polarization.[6] For example, in the case of rotation by 90° and spherical optics ($\alpha_\| = \alpha_\perp = \alpha$), the relevant boundary conditions are [compare with Eq. (13)]

$$B_4(x, z) = \left(\frac{T}{\alpha^2} \right)^{1/2} B_2\left(\frac{z}{\alpha}, \frac{x}{\alpha} \right),$$

$$B_{1,in}(y, z) = (T\alpha^2)^{1/2} B_{3,out}(\alpha z, \alpha y) \tag{26}$$

and they yield the following equation for the eigenfunction Ψ [compare with Eq. (19)]:

$$\Psi(x, z) = \int dx' \, K(x, x', z) \Psi(\alpha z, x'), \tag{27}$$

where K is a certain kernel.

The analysis of Eq. (27) carried out in Ref. 6 shows that the boundary conditions of Eq. (26) ensure selection of the phase-conjugate component for any value of the scaling coefficient α.

We shall now list the most important theoretical conclusions.

1) The physical mechanisms responsible for the formation of the scattered radiation in the beam-intersection plane are qualitatively different from those transverse to this plane.

2) Phase conjugation in a loop parametric oscillator is possible in the limit of high Fresnel numbers if the secondary pump beam 4 in the interaction region at right-angles to the beam-intersection plane is narrower than the primary pump beam 2: $\alpha_\perp < 1$. The relationship between the widths of these beams in the beam-intersection plane can be arbitrary.

3) The quality of phase conjugation increases with the scaling coefficients $\alpha_\perp$ and $\alpha_\|$. The optimal quality corresponds to values of these coefficients near unity, but in the limit $\alpha_\perp \to 1$ we can expect excitation not only of the fundamental mode, but also of higher transverse modes because of the proximity of their thresholds (Fig. 2).

4) For $\alpha_\perp \to 1$, the scattered beam is not phase-conjugated. The radius of curvature of its wavefront transverse to the beam-intersection plane is given by Eq. (9).

5) Phase conjugation in a loop oscillator system may be achieved by rotation of the transverse cross section of the beam propagating along the feedback loop, provided the angle of rotation differs from zero and 180°. Phase conjugation then occurs for any ratio of the pump beam diameters.

3. EXPERIMENTS

The system shown schematically in Fig. 1 was assembled in order to investigate experimentally the spatial structure of the scattered radiation in a loop parametric oscillator. We used a helium–neon laser ($\lambda = 0.63$ μm) of ≈ 10 mW power emitting the TEM$_{00}$ mode. A collimated laser beam ≈ 3 mm in diameter was directed to a cerium-doped strontium–barium niobate (SBN) crystal whose thickness was ≈ 3 mm. After passing through this crystal, the beam was rotated by two metal mirrors and returned to the crystal at an angle of $\sim 35°$ (in air) relative to its previous direction of propagation. (For the selected beam diameters and the angle between them the beam-intersection region was only partly inside the crystal, which was not quite in agreement with the theoretical model.) The optic axis of the crystal was parallel to its entry face and was in the beam-intersection plane. The incident laser radiation was polarized in the same plane. This geometry made it possible to utilize the largest electrooptic coefficient r_{33} of the crystal. The radii of curvature of the wavefronts and the beam diameters were altered by placing lenses in the feedback loop.

Investigation of the structure of the back-reflected radiation showed that it depended qualitatively only on the ratio $\alpha = d_4/d_2$ of the diameters of the secondary (d_4) and primary (d_2) pump beams in the crystal. When this ratio was
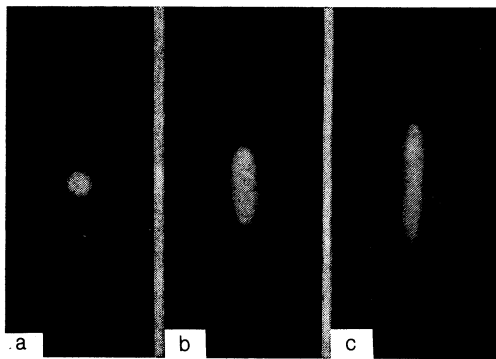
FIG. 3. Structure of the back-reflected beam recorded in the far-field zone as a function of $\alpha = \alpha_{\parallel} = \alpha_{\perp}$. The value of α increases from a to c: a) $\alpha < 1$; b), c) $\alpha > 1$.

FIG. 5. Structure of the reflected beam in far-field zone: a) $\alpha_{\perp} = \alpha_{\parallel} = \alpha \approx 1.5$; b) $\alpha_{\parallel} = 0.9$, $\alpha_{\perp} \approx 1.5$; c) $\alpha_{\parallel} \approx 1.5$, $\alpha_{\perp} \approx 0.9$.

$\alpha < 1$, the distribution of the intensity in the back-reflected beam was a circular spot in the far-field zone and its divergence was close to the divergence of the pump beam (Fig. 3a). For $\alpha > 1$, the beam had an oval shape (Figs. 3b and 3c) elongated per perpendicular to the beam-intersection plane inside the crystal. The beam divergence in this direction depended on the diameter and radius of curvature of the wavefront of the secondary pump beam, whereas the divergence in the beam-intersection plane was close to the divergence of the incident pump beam. Such a dependence of the structure of the back-reflected beam on the parameter α had been reported earlier for a loop parametric oscillator utilizing stimulated Brillouin scattering.[10-12]

The reflected beam was investigated under conditions when it was not the phase conjugate of the pump beam ($\alpha > 1$) by placing a lens with a focal length $f = 64$ mm inside the feedback loop. The distance from this lens to the crystal along the direction of propagation of the laser beam was greater than twice its focal length, ensuring $\alpha > 1$. A change in the length L_2 made it possible to alter the value of α. The dependence of the radius of curvature of the wavefront of the back-reflected beam is plotted in Fig. 4 as a function of α for the direction perpendicular to the beam-intersection plane and two values of the total feedback loop length. The continuous curves represent the results obtained using the theoretical expressions in Eq. (9) on the assumption that $R_2 = \infty$, whereas the points are the experimental values.

A separate investigation of the role of the beam-intersection plane and of the direction perpendicular to it in the formation of the scattered radiation was carried out using a system of two lenses. A negative (diverging) spherical lens was placed in the feedback loop to ensure $\alpha > 1$, whereas a positive (converging) cylindrical lens placed behind the spherical lens made it possible to alter the scaling coefficient either in the beam-intersection plane ($\alpha_{\parallel}$) or at right-angles to this plane ($\alpha_{\perp}$) without altering the value of this coefficient along the second direction. The experimental results (Fig. 5) show that phase conjugation was possible when the pump beam was compressed only perpendicular to the beam-intersection plane.

One further prediction of the theory was checked by placing in the feedback loop a system of prisms which rotated the transverse cross section of the beam by 90°. The polarization rotator then returned the polarization of the beam to the intersection plane. Under these conditions (Fig. 6) the divergence of the back-reflected beam remained close to the divergence of the pump beam even for $\alpha > 1$.

According to the theory, the excitation thresholds of the higher transverse modes should be close to the threshold of the fundamental mode if α is close to unity. Such modes were observed experimentally for $\alpha \approx 0.9$ during the transient stage of the operation. The transverse modes were ex-
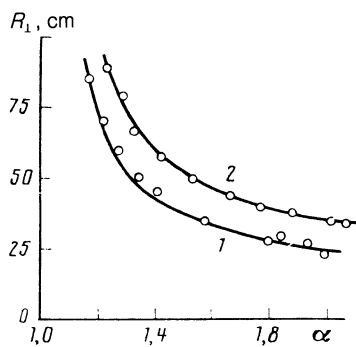

FIG. 4. Dependence of the radius of curvature of the wavefront of the reflected beam at right-angles to the beam-intersection plane on $\alpha = \alpha_{\parallel} = \alpha_{\perp}$ when $\alpha > 1$, plotted for two lengths of the feedback loop: 1) $L = 48$ cm; 2) $L = 56$ cm. The points are the experimental results and the continuous curves are theoretical.
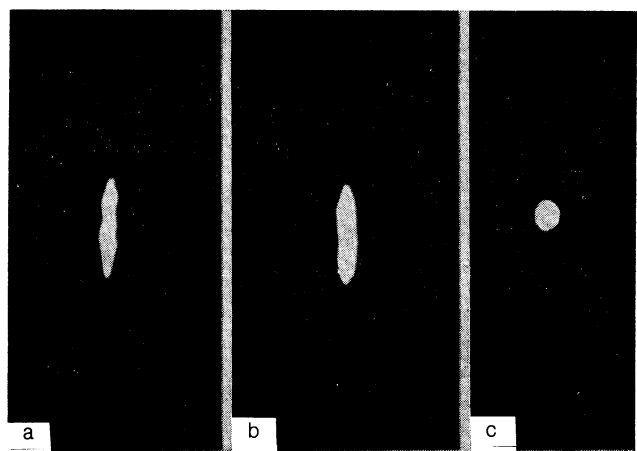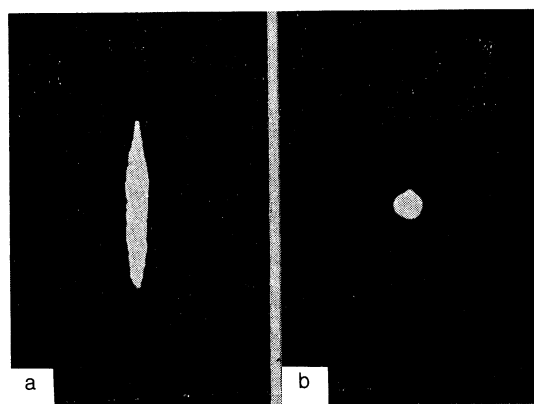

FIG. 6. Structure of the reflected beam plotted for $\alpha_{\parallel} = \alpha_{\perp} = \alpha \approx 1.5$ (a) and for the same value of α, but after rotation of the transverse cross section of the beam by 90° (b).
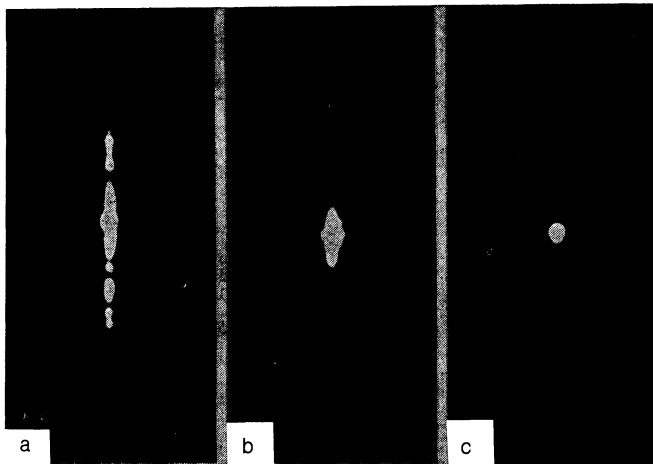
FIG. 7. Structure of the reflected beam in the case when $\alpha_\parallel = \alpha_\perp = \alpha \approx 0.9$: a) $t \approx 2$ min; b) $t \approx 4$ min; c) $t \approx 10$ min.
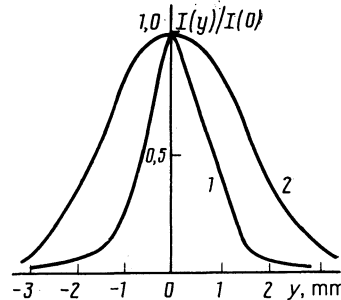

FIG. 8. Distribution of the intensity in the cross sections of the beams recorded in the plane of the face of the investigated crystal for $\alpha \approx 0.5$: 1) reflected beam; 2) pump beam.

cited first (Fig. 7a), but after a certain time (Fig. 7b) only the fundamental mode with the lowest threshold survived (Fig. 7c). As a rule, for $\alpha \leqslant 1$ the scattered radiation appeared directly in the form of a bright spot and the pattern shown in Fig. 7 was not observed. It was possible, however, to record it by ensuring a careful imaging of the face of a crystal on itself, which ensured a short effective length of the feedback loop.

Finally, we determined the distribution of the intensity over the cross section of the reflected beam at the exit from the crystal for $\alpha \approx 0.5$ (curve 1 in Fig. 8). For comparison, we also determined the distribution of the pump intensity (curve 2). For this value of α the reflected beam was narrower than the pump beam. For $\alpha \approx 1$, the distribution of the intensity in the reflected beam was practically identical with the distribution of the pump beam, indicating that the quality of phase conjugation increased as a function of the parameter α. In contrast to the experimental predictions, there was no significant difference between the experimental distributions of the intensity in the reflected beam in the beam-intersection plane and perpendicular to this plane. This was due to the fact that in our experiments the beam-intersection region was only partly inside the photorefractive crystal.

4. CONCLUSIONS

We carried out a detailed experimental investigation of the structure of the scattered radiation in the geometry of a loop parametric oscillator utilizing a photorefractive crystal (Fig. 1) and compared the results with the predictions of the three-dimensional model developed in Refs. 6 and 7. According to this model, the main theoretical parameters governing the structure of the scattered beam in a loop oscillator in the case of large Fresnel numbers are the scaling transfor-

mation coefficients $\alpha_\parallel$ and $\alpha_\perp$ of the pump beams in the plane of their intersection and perpendicular to this plane. In practice the scaling coefficient $\alpha_\parallel$ is equal to the ratio of the width of the secondary pump beam 4 in the beam-intersection plane to the width of the pump beam 2. For $|\alpha_\parallel| < 1$ the pump beam 4 is narrower than the beam 2, whereas the reverse is true if $|\alpha_\parallel| > 1$. This applies also to the scaling coefficient $\alpha_\perp$, but perpendicular to the beam-intersection plane. The most important theoretical predictions are given at the end of the theoretical section. Experimental investigations of the spatial structure and dynamics of formation of the scattered beam, carried out under conditions corresponding to different values of $\alpha_\parallel$ and $\alpha_\perp$, agree with the theoretical predictions.

[1] V. I. Odintsov and L. F. Rogacheva, Pis'ma Zh. Eksp. Teor. Fiz. 36, 281 (1982) [JETP Lett. 36, 344 (1982)].

[2] M. Cronin-Golomb, B. Fischer, J. O. White, and A. Yariv, IEEE J. Quantum Electron. QE-20, 12 (1984).

[3] T. V. Galstyan and A. V. Sukhov, Zh. Tekh. Fiz. 60(3), 81 (1990) [Sov. Phys. Tech. Phys. 35, 321 (1990)].

[4] A. A. Zozulya and V. T. Tikhonchuk, Kvantovaya Elektron. (Moscow) 15, 1570 (1988) [Sov. J. Quantum Electron. 18, 981 (1988)].

[5] M. G. Zhanuzakov, A. A. Zozulya, and V. T. Tikhonchuk, Kvantovaya Elektron. (Moscow) 16, 379 (1989) [Sov. J. Quantum Electron. 19, 254 (1989)].

[6] A. A. Zozulya, V. P. Silin, and V. T. Tikhonchuk, Zh. Eksp. Teor. Fiz. 92, 788 (1987) [Sov. Phys. JETP 65, 443 (1987)].

[7] A. A. Zozulya, V. P. Silin, and V. T. Tikhonchuk, Zh. Tekh. Fiz. 58, 1331 (1988) [Sov. Phys. Tech. Phys. 33, 792 (1988)].

[8] Yu. A. Anan'ev, Optical Resonators and the Problem of Divergence of Laser Radiation [in Russian], Nauka, Moscow (1979).

[9] V. V. Eliseev, A. A. Zozulya, and V. T. Tikhonchuk, Zh. Eksp. Teor. Fiz. 99, 68 (1991) [Sov. Phys. JETP 72, 35 (1991)].

[10] O. P. Zaskal'ko, A. A. Zozulya, N. N. Panaioti, and V. T. Tikhonchuk, Kratk. Soobshch. Fiz. No. 8, 43 (1986).

[11] I. Yu. Anikeev, I. G. Zubarev, and S. I. Mikhaĭlov, Kvantovaya Elektron. (Moscow) 13, 2320 (1986) [Sov. J. Quantum Electron. 16, 1529 (1986)].

[12] V. V. Eliseev, N. N. Zhukov, O. P. Zaskal'ko et al., Izv. Akad. Nauk SSSR Ser. Fiz. 52, 393 (1988).

Translated by A. Tybulewicz